

Sensorimotor synchronization: neurophysiological markers of the asynchrony in a finger-tapping task

Luz Bavassi^{1,2}  · Juan E. Kamienskowski^{1,3} · Mariano Sigman^{1,4} · Rodrigo Laje⁵

Received: 27 February 2015 / Accepted: 22 October 2015
© Springer-Verlag Berlin Heidelberg 2015

Abstract Sensorimotor synchronization (SMS) is a form of referential behavior in which an action is coordinated with a predictable external stimulus. The neural bases of the synchronization ability remain unknown, even in the simpler, paradigmatic task of finger tapping to a metronome. In this task the subject is instructed to tap in synchrony with a periodic sequence of brief tones, and the time difference between each response and the corresponding stimulus tone (asynchrony) is recorded. We make a step towards the identification of the neurophysiological markers of SMS by recording high-density EEG event-related potentials and the concurrent behavioral response-stimulus asynchronies during an isochronous paced finger-tapping task. Using principal component analysis, we found an asymmetry between the traces for advanced and delayed responses to the stimulus, in accordance with previous behavioral observations from perturbation studies.

We also found that the amplitude of the second component encodes the higher-level percept of asynchrony 100 ms after the current stimulus. Furthermore, its amplitude predicts the asynchrony of the next step, past 300 ms from the previous stimulus, independently of the period length. Moreover, the neurophysiological processing of synchronization errors is performed within a fixed-duration interval after the stimulus. Our results suggest that the correction of a large asynchrony in a periodic task and the recovery of synchrony after a perturbation could be driven by similar neural processes.

Introduction

Synchronization of motor actions to an external pacing signal, also known as sensorimotor synchronization (SMS), is a crucial ability for many behaviors that are mostly specifically human, like music and dance (Repp 2005; Repp & Su 2013). In the model task of finger tapping to a beat, subjects are able to maintain average synchrony even if no single response is perfectly aligned in time with the corresponding stimulus (Fig. 1a). Synchronization errors or asynchronies are defined as the time difference between the occurrences of each tap and the corresponding tone. Asynchronies are typically in the range of tens of milliseconds (Pressing & Jolley-Rogers 1997; Chen, Ding, & Kelso, 2001; Repp & Penel 2002). It is readily accepted that accurate temporal precision in this task relies at least in part on the existence of an error correction mechanism for the asynchronies (Michon & Van der Valk 1967; Hary & Moore 1987; Repp & Su 2013). In the last years the number of publications looking for brain regions involved in finger tapping has increased. Pollok, Gross, Kamp & Schnitzler (2008) found evidence

✉ Luz Bavassi
luzbavassi@gmail.com

¹ Departamento de Física, FCEyN, UBA and IFIBA-CONICET, Pabellón 1, Ciudad Universitaria, Buenos Aires 1428, Argentina

² Laboratorio de Neurobiología de la Memoria, Departamento de Fisiología, Biología Molecular y Celular, FCEyN, UBA and IFIBYNE-CONICET, Buenos Aires, Argentina

³ Laboratorio de Inteligencia Artificial Aplicada, Departamento de Computación, FCEyN, UBA, Buenos Aires, Argentina

⁴ Universidad Torcuato Di Tella, Almirante Juan Saenz Valiente 1010, Buenos Aires C1428BIJ, Argentina

⁵ Departamento de Ciencia y Tecnología, Universidad Nacional de Quilmes, Argentina, and CONICET Argentina, Buenos Aires, Argentina

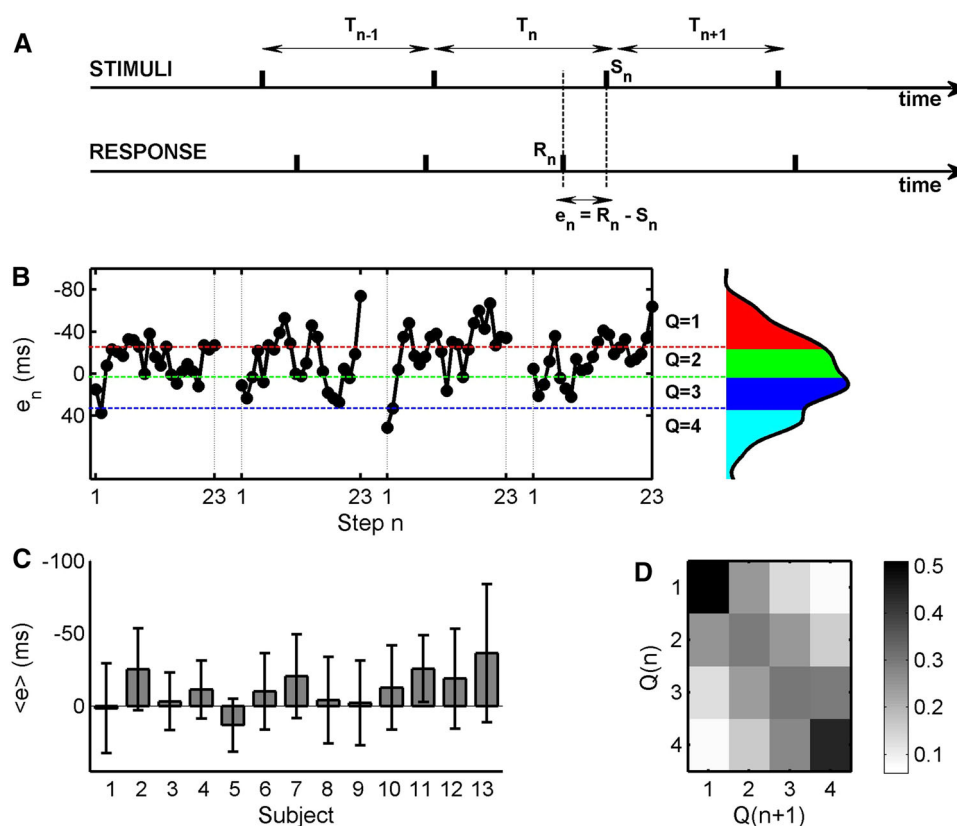


Fig. 1 Task and behavior. **a** Schematic of behavior and definition of variables. The asynchrony is the time difference between response and stimulus $e_n = R_n - S_n$. **b** Four typical time series from one subject and distribution of asynchronies e_n from all the subject's sequences. Colors (red, green, blue, cyan) represent the four asynchrony subsets $Q = 1, 2, 3, 4$ (separated by the 25, 50, and 75 % percentiles). **c** Average asynchrony for each subject sorted by hours of musical training per week (subjects 1–2: more than 25 h per week;

subjects 3–5: between 15 and 25 h; subjects 6–10: between 5 and 15 h; subjects 11–13: less than 5 h). Note there is a tendency to anticipation, called negative mean asynchrony (NMA). **d** Transition probability matrix between quartiles at consecutive responses $Q(n)$ and $Q(n+1)$ (all sequences from all subjects pooled). For every row or column, the largest probability occurred in the diagonal element and decreased towards the borders (t -test, $p < 2.10^{-4}$). All the data refer to $T_n = 667$ ms

that a cerebello-diencephalic-parietal loop might be crucial for anticipatory motor control, whereas parietal–cerebellar interaction might be critical for feedback processing. Besides, Bijsterbosch et al. (2011) showed that suppression of the left but not the right cerebellum with theta-burst Transcranial Magnetic Stimulation (TMS) significantly affected error correction of supraliminal phase-shift perturbations, demonstrating necessary involvement of the cerebellum in the correction process. However, there are other explanations related to non-temporal processes to account for the cerebellum's involvement in rhythmic timing tasks, like for instance the hypothesis that impairments of speed, precision and timing of movements would not be due to a faulty cerebellar “timekeeper” but to the lack of available high-quality sensory data (see Molinari, Leggio, & Thaut 2007 for a review). Beyond the advance in the topic, the specific dynamics of the error correction mechanism(s), such as the higher processing of the asynchrony, remains unknown.

A number of well-established behavioral observations help in the building hypotheses about the inner workings of this mechanism. In an isochronous, auditory paced finger-tapping task, the asynchrony distribution is typically Gaussian, with a tendency to tap anticipation called Negative Mean Asynchrony or NMA (Aschersleben 2002). Both the standard deviation and mean (in absolute value) of asynchronies increase linearly as the interstimulus interval is increased (Repp 2003), which can lead to the hypothesis that the processing of synchrony errors is done relative to the period of the stimulus sequence. An alternative hypothesis would be that the processing of errors is performed within a time window with a more or less fixed duration after the stimulus, irrespective of the interstimulus period. This alternative hypothesis is based on results from error-related negativity (ERN) studies where the latency of the ERN was shown to be independent of the speed of the corrective response (Rodríguez-Fornells, Kurzbuch, & Münte 2002).

Notably, the recovery of average synchrony after a perturbation is asymmetric—positive and negative perturbations of the same magnitude do not elicit similar recoveries. Indeed, Thaut, Tian & Azimi-Sadjadi (1998) showed that the recovery after a negative step-change perturbation (an abrupt decrease of 10 % in tempo) was a monotonic exponential convergence to the new baseline, but after a positive perturbation the recovery displayed an overshoot. Moreover, Bavassi, Tagliazucchi & Laje (2013) showed that the overshoot asymmetry was present even for smaller perturbation magnitudes up to around the detection threshold (i.e., subliminal). Asymmetries were also reported for phase-shift perturbations, although only for larger perturbation magnitudes of 10 % and above (Repp 2002, 2011). The observed asymmetries could be associated with asymmetries in the neural mechanisms driving the behavior, in principle at any level from a differential perception of negative and positive asynchronies, to a differential processing of positive and negative errors, to a differential activation of the effector for speeding-up and slowing-down corrective responses (Praamstra, Turgeon, Hesse, Wing, & Perryer 2003). It might be expected, then, that these asymmetries show up in the neurophysiological traces, including any asymmetry in the putative error signal. Indeed, Praamstra et al. (2003) showed that an error-related negativity (ERN) occurred only after large, positive phase-shift perturbations. However, it is still unclear whether an asymmetry in the neurophysiological traces would be found in an isochronous task, where there are no perturbations but only normally occurring positive and negative asynchronies.

In this work we recorded high-density electroencephalographic (EEG) event-related potentials (ERPs) and the concurrent behavioral asynchronies during an isochronous paced finger-tapping task. Our aim is to characterize the neurophysiological markers of the processing of synchrony errors to make a step forward in the explanation of the error correction mechanism.

Materials and methods

Participants

Thirteen participants performed the experiment (12 male/1 female, age range 20–31 years). All participants were right handed and had musical training [thus displaying less timing variability and smaller NMA, in line with the previous study (Bavassi et al. 2013)]. Five of them played guitar, six played the piano, one played bass guitar, and one played percussion instruments. All participants had normal audition and gave written informed consent. All subjects had at least 2 years of uninterrupted musical training. The

experiment described in this paper was reviewed and approved by the Comité de Ética del Centro de Educación Médica e Investigaciones Clínicas “Norberto Quirno” (CEMIC, Argentina), certified by the Department of Health and Human Services (HHS, USA): IRb00001745-IORG 0001315, as stated in Protocol #435, December 10th, 2007.

Experiment

Participants were presented with periodic sequences consisting of 30 auditory stimuli (29 periods). Each stimulus consisted of a 50-ms duration square-wave tone (440 Hz). Sequence period was either $T_n = 667$ ms (sequence duration 19.3 s) or $T_n = 444$ ms (sequence duration 13.3 s). There were two conditions: a test condition in which participants were instructed to tap and keep pace with the auditory stimulus, and a passive condition where participants only listened to the stimuli sequence. In this work we only studied the tapping condition. There were 24 sequences of each condition; total number of sequences was 96 (=24 × 2 conditions × 2 periods), presented in random order. Before starting each sequence, a screen showed the corresponding sequence’s instruction (tap/listen) and participants had to press a key on the keyboard using their left hand; the actual sequence started at a random time after the key press (range 1–2 s). Tapping was performed always with the right hand. Participants were instructed to perform the task with closed eyes to avoid eye blink artifacts. Subjects were free to rest and blink during the pause between sequences. The pause length was not restricted.

Apparatus

Participants sat in a comfortable chair; stimuli were presented through two speakers located 80 cm in front of the participant, symmetrically located on each side. Responses were detected as a voltage spike produced by the subject tapping on a copper plate with his/her right index finger, with no additional auditory feedback from the taps. Stimulus generation and response detection were performed with Arduino (<http://www.arduino.cc/>), an open-source electronics prototyping platform yielding a time resolution of 1 ms. Every time Arduino played a stimulus or detected a tap, it saved the absolute time of occurrence of both stimulus and response, and sent a synchronization mark to an external channel on the EEG. The microcontroller on the Arduino board was programmed in C using the Arduino development environment. Arduino communicated with a computer using MATLAB (Mathworks, Natick, MA) and PsychToolbox (Brainard 1997) through a USB serial port at the beginning and at the end of each sequence. Interfacing and signal conditioning (e.g., socket for headphone mini-

plug, volume adjustment) was performed on a custom-made Arduino “shield” (a board that can be plugged on top of the Arduino; schematic available on request).

Behavioral data

Our main variable of interest was the asynchrony (e_n), defined as the time difference between each response and the corresponding stimulus (Fig. 1a). In order to avoid transient effects and to cut the EEG data as described in “EEG data acquisition and preprocessing” we excluded the first four and the last three stimuli from each sequence; thus each analyzed sequence consisted of 23 stimuli (Fig. 1b). In addition to this, we discarded the sequences with missing taps or with asynchronies greater than 50 % of the period.

In order to explore the correlation between electrophysiological traces and behavioral asynchronies we grouped the asynchronies into four subsets (within each subject). The asynchrony subsets ($Q = 1, 2, 3, 4$) were based on a quartile split ([0;25 %], [25 %;50 %], [50 %;75 %] and [75 %;100 %] of each subject’s distribution, between 120 and 143 epochs per quartile). Consecutive taps had in general different asynchronies, so that we defined the transition probability between asynchrony subsets from consecutive taps $Q(n)$ and $Q(n + 1)$, where $Q(n)$ is the asynchrony subset at time $t = 0$ and $Q(n + 1)$ is the subset at the following step.

EEG data acquisition and preprocessing

EEG activity was recorded on a dedicated PC at 1024 Hz sampling frequency, at 128 electrode positions on a standard 10–20 montage, using the Biosemi Active-Two system (Biosemi, Amsterdam, Holland, <http://www.biosemi.com/products.htm>). Four extra electrodes were placed at both mastoids and ear lobes. After data were recorded, it was digitally downsampled to 512 Hz using a fifth-order sinc filter to prevent aliasing, and imported into MATLAB using the EEGLAB toolbox (Delorme & Makeig 2004) using the right ear lobe channel as voltage reference. The data were filtered between 1 and 40 Hz (4th-order elliptic high-pass filter and 10th-order elliptic low-pass filter, respectively) to discard slow oscillatory trends, high-frequency noise, and periodic artifacts like heartbeat. Bad channels were detected by visual inspection of the raw data and the spectra, and replaced by an interpolated signal using all the other channels weighted by the inverse distance to the replaced channel. This was necessary for one or two channels in 7 subjects. The continuous EEG recordings were segmented into overlapping epochs spanning six periods, with $t = 0$ the center stimulus in each epoch (if stimulus-aligned) or the center response in each

epoch (if response-aligned). We excluded epochs with no response or when the time difference between the tap and tone was greater than 50 % of the period (in absolute value). Prior to data analysis, the resulting epochs were re-referenced to the corresponding epoch average.

The following pre-analysis was performed as in Kamienkowski, Ison, Quiroga, & Sigman (2012). To further eliminate artifacts we applied an amplitude threshold of 80 μ V to each channel \times epoch. If less than 5 channels in any given epoch exceeded the threshold, those channels were interpolated in that single epoch; and if more than 5 channels in one epoch exceeded the threshold the epoch was rejected. The average number of epochs after all rejections was between 540 and 552 per subject.

Finally, to remove the high-power alpha oscillation (subjects performed the task with closed eyes), we used a notch filter (width ± 1 Hz) around the alpha peak for each subject. In every case, alpha peak was between 9 and 11 Hz.

We performed an Independent Component Analysis (ICA: Makeig, Bell, Jung & Sejnowski 1996) together with an automatic algorithm that identifies artifacts (ADJUST: Mognon, Jovicich, Bruzzone, & Buiatti 2011) to discard eye movements. From the original basis of 128 components a set of 15 ± 5 were discarded.

Principal component analysis (PCA)

PC decomposition

We calculated the principal components for the grand-average data for both periods and kept with the first two principal components (PC) that resulted from the projection of the epoched ERPs (Duda, Hart, & Stork 2000). Then we projected all epochs onto the obtained PCs (Sigman & Dehaene 2008), and grouped the resulting time series based on the corresponding behavioral asynchrony subsets $Q = 1, 2, 3, 4$.

Latency analysis

The time series of the obtained PCs displayed peaks and valleys (Figs. 3d, f and 4d, f). In order to analyze the correlation between PC latency and behavioral asynchrony, we defined latency as the first time the trace crossed a threshold towards its first peak. To this end, we searched for a crossing within a time window between -5 and 300 ms; the thresholds were defined as 50 % of the peak value of the averaged $Q = 1$ subset (upward going for PC1, downward going for PC2). The results presented here were not dependent on the particular percentage value—threshold values from 35 % through 65 % yielded similar results.

Jump versus no-jump transitions

For our analysis spanning two consecutive stimuli of PC2, we grouped the data according to whether the recorded asynchrony stayed in the same subset Q at consecutive steps n and $n + 1$ or changed subset (“jump” or “no jump”, see schemes in Fig. 5). To include only the largest jumps, we discarded transitions between adjacent subsets and considered jumps originating from the extreme subsets only. Together, the four groups were: $Q(n) = 1$ and $Q(n + 1) = 1$ (“no jump”); $Q(n) = 1$ and $Q(n + 1) = 3$ or 4 (“jump”); $Q(n) = 4$ and $Q(n + 1) = 4$ (“no jump”); $Q(n) = 4$ and $Q(n + 1) = 1$ or 2 (“jump”).

Statistical analysis

Comparisons among channel time series for asynchrony subsets

In order to compare the scalp activations across asynchrony subsets at chosen timepoints after stimulus occurrence (Fig. 2b), we used the cluster-based permutation test implemented in FieldTrip package (Maris & Oostenveld 2007), corrected for (channel time)-multiple comparisons. This is a non-parametric statistical test, based on clustering of adjacent (channel, time)-samples that exhibit a significant difference and have the same sign. Clusters consisted of 3 adjacent channels and all time points in the epoch. p values are approximated by a Monte Carlo method, obtained by making 1000 random partitions and then comparing these random test statistics with the observed test statistic (critical alpha-level was 0.05). We used the option ‘depsamplesF’ to perform an overall comparison among the four asynchrony subsets (F -statistic), and option ‘depsamplesT’ to perform partial comparison among selected subsets (t -statistic, Bonferroni-corrected post hoc).

Comparisons among PC projections

For all the time series shown in Figs. 3, 4, and 5, comparisons among asynchrony subsets were performed in a pairwise fashion (i.e. within-subject design), using a permutation test implemented in the function `statcond` from the EEGLAB package [EEGLAB toolbox, (Delorme & Makeig 2004)]. This function runs a one-way, repeated-measures ANOVA (with factor $Q(n)$, 4×1 in Figs. 3d, f, 4d, f; factor $Q(n + 1)$, 2×1 in Fig. 5) on each time-sample for 1000 permuted data sets, and the p value is calculated as the proportion of significant tests (with critical alpha-level = 0.05). In order to avoid spuriously significant results from isolated timepoints, we considered a timepoint significant when $p < 0.01$ for 10 consecutive timepoints following it (19 ms, black line, Figs. 3, 4) or

$p < 0.05$ for 8 consecutive timepoints (17 ms, gray line, Fig. 5) (Dehaene et al. 2001; Kamienkowski et al. 2012).

Comparisons among single peaks

To compare the amplitude of the negative peak of PC2 across asynchrony subsets (Fig. 4d, f), we measured the amplitude of the absolute peak between 50 ms and 200 ms per subject and performed a one-way, 4×1 ANOVA using subsets $Q(n)$ as independent variable and subjects as random variable (critical alpha-level of 0.05, and Bonferroni correction for multiple post hoc comparisons).

Comparisons for a single time-window

We also used a global permutation test (Hemmelmann et al. 2004) to assess differences between “jump” and “no jump” traces in a fixed time window (Fig. 5). The p -value is calculated as the proportion of significant tests among 1000 permutations (with critical alpha-level = 0.05). In this case we computed a t -statistic for each time point within a fixed time window and then kept the maximum absolute t -value (t_{\max}) in each permutation. We compared the positive-going ramp of PC2, between 300 ms and the interstimulus period plus the mean asynchrony of $Q = 1$ to avoid the response occurrence (between 300 and 441 ms for the shorter period and between 300 and 625 ms for the longer period).

Comparisons among ramp onsets

To compare the time occurrences of the onset of the positive-going ramp for PC2 (Fig. 6), we performed a three-way, $2 \times 2 \times 2$, repeated measures ANOVA with factors $Q(n)$ (1, 4), transition (jump/no jump), and period (667, 444 ms). We defined ramp onset as the time when the minimum value occurs during a time window between $t = 150$ and $t = 400$ ms.

Results

Behavior

Figure 1b displays four sample series from one subject (left panel), and the distribution of all asynchronies from the same subject for $T_n = 667$ ms (right panel). The distribution of asynchronies was not significantly different from a Gaussian for every subject (Kolmogorov–Smirnov test, $p > 0.05$). Eleven out of the thirteen subjects displayed the expected NMA. Mean asynchrony is shown in Fig. 1c, with subjects ordered by number of hours per week devoted to musical training.

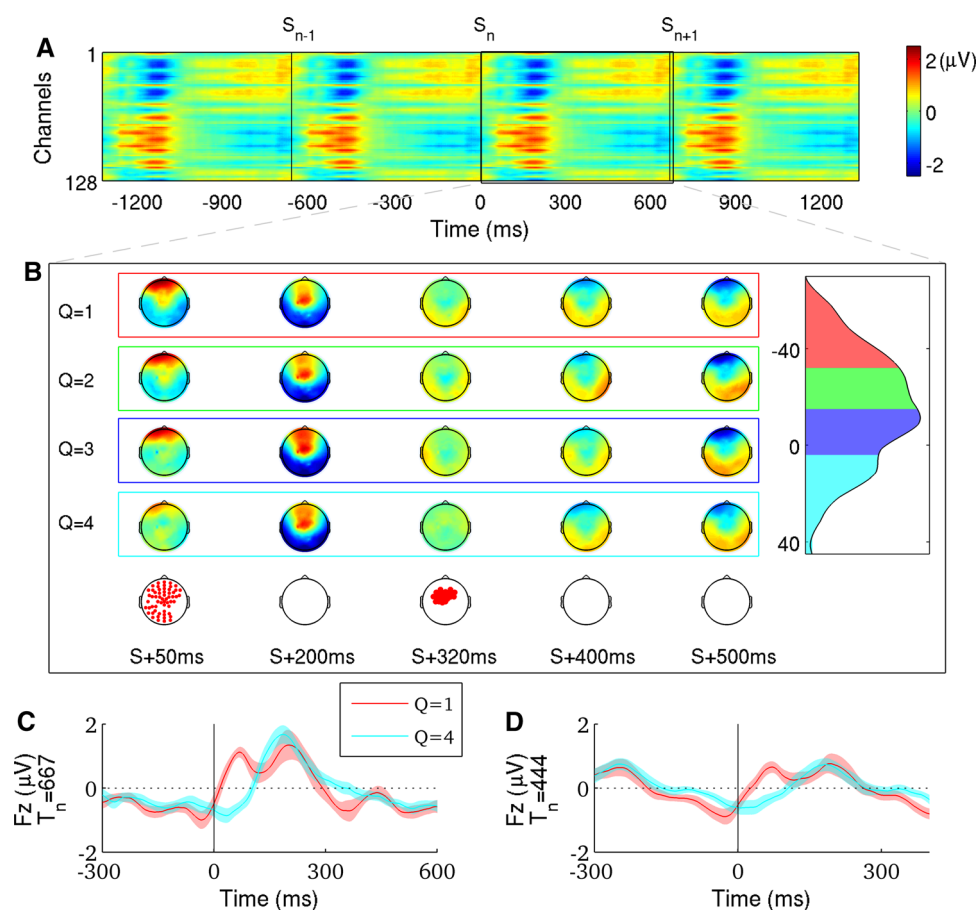


Fig. 2 Grand-averaged EEG data (across trials and subjects). **a** Color-coded activity at each electrode site. Epochs spanned six periods (only four pictured here); data was locked to the stimulus occurrence. $T_n = 667$ ms. **b** Average of scalp voltage distributions at $t = 50$, $t = 200$, $t = 320$, $t = 400$ and $t = 500$ ms after the stimulus occurrence, for each asynchrony subset $Q = 1, 2, 3, 4$ at $t = 0$ (first four rows). Last row displays channels with significant differences across rows at $t = 50$ ms (F -statistic, Comparisons among channel

time series for asynchrony subsets, $p < 0.0001$) and $t = 320$ ms (F -statistic, comparisons among channel time series for asynchrony subsets, $p < 0.05$). $T_n = 667$ ms. **c, d** Potential at a frontal site (Fz) for $T_n = 667$ ms and $T_n = 444$ ms, respectively. The Fz time series was averaged across a pool of 5 neighboring electrodes around Fz; red trace is the time series of the negative asynchronies ($Q = 1$), cyan trace is $Q = 4$ time series

For further analysis, we grouped the data into four subsets $Q = 1, 2, 3, 4$ based on a quartile split ($Q = 1$ corresponds to the most negative asynchronies, $Q = 4$ corresponds to the most positive asynchronies; see “Materials and methods” and Fig. 1b). The transition probability between consecutive taps is displayed in Fig. 1d, which reveals a clear tendency to persist in the current asynchrony subset: higher transition probabilities in the diagonal of the transition matrix compared to non-diagonal elements. Note that this is not in disagreement with the well-known result of negative lag-1 autocorrelation of the interresponse intervals (Wing & Kristofferson 1973a, b), as our work deals with a different parameter. Transition probability is lower for transitions to or from subsets farther apart (i.e. for every row or column, the largest probability occurs in the diagonal element and decreases towards the borders). This can be seen after performing a linear regression between

transition distance $|Q(n + 1) - Q(n)|$ and transition probability for each subject; we found that the slope was always negative (t -test, $p < 2.10^{-4}$ for every slope). The slopes themselves were not significantly different, and in particular slopes for transitions towards and away from the median were not different, in agreement with previous reports which do not inform of any asymmetrical behavioral features in isochronous sequences (Pressing & Jolley-Rogers 1997).

Event-related EEG potentials

The synchronization behavior elicits very clear, periodic, and stereotypical activations. As an example for period $T_n = 667$ ms, at 200 ms after the stimulus we observed a strong activation in almost all electrodes (positive for frontal regions and negative for occipital regions). These

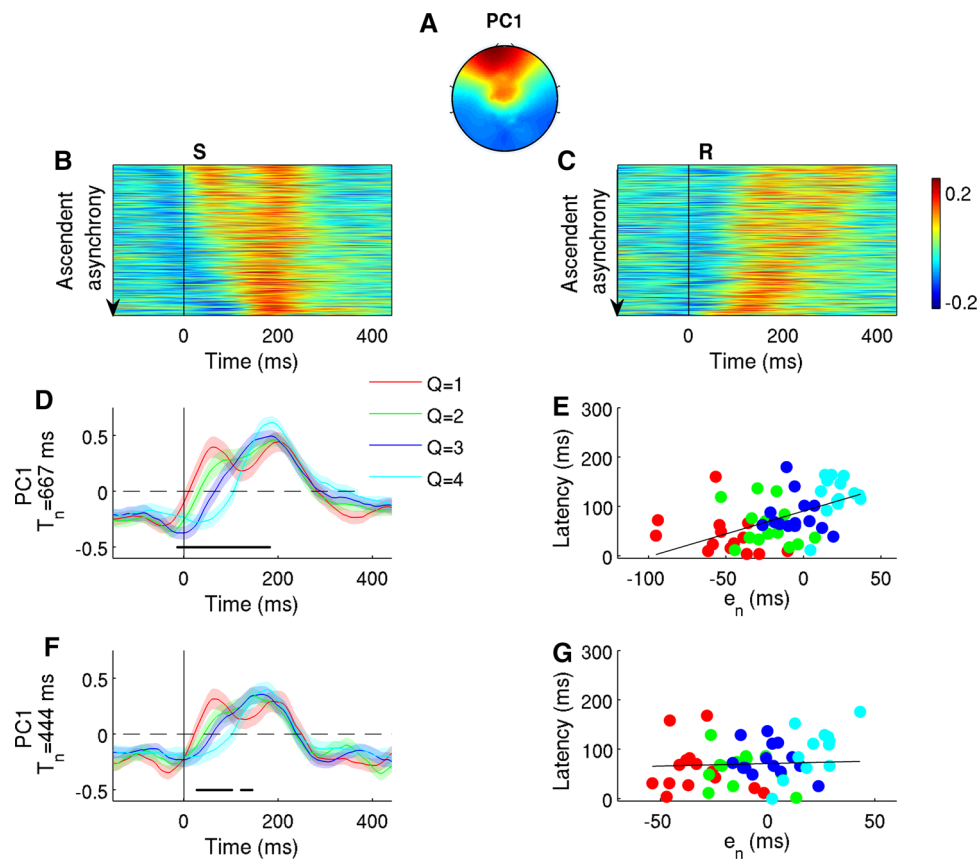


Fig. 3 The first principal component (PC1) is a combined component for stimulus- and response-locked potentials. **a** Scalp topography of PC1 for $T_n = 667$ ms. PC1 accounted for 91 % of the variance. **b**, **c** PC1 activations from stimulus- and response-aligned data for $T_n = 667$ ms (projection of all epochs sorted by increasing asynchrony and averaged across subjects). **d**, **f** PC1 activations grouped by asynchrony subset for $T_n = 667$ ms and $T_n = 444$ ms, respectively (*thick line* mean; *shaded region* standard error). Stimulus-aligned data, projected onto PC1 and averaged within asynchrony subsets and

across all subjects. The *solid black horizontal segments* identify time windows where the difference between traces was significant (comparisons among PC projections, $p < 0.01$ during 19 ms, see “[Materials and methods](#)”). **e**, **g** Correlation between median of asynchrony subset and PC1 first peak latency for $T_n = 667$ ms and $T_n = 444$ ms, respectively. The correlation between latency and median of asynchronies was significant for the longer period ($R^2 = 0.57$, $p < 0.001$) and not significant for the shorter period ($R^2 = 0.15$, $p = 0.07$)

activations gradually changed sign during the remainder of the period peaking near the time of the next stimulus (Fig. 2a).

The voltage scalp distribution for the longer period sequences showed large differences among asynchrony subsets near the stimulus occurrence (between -15 and 140 ms), as illustrated by the first column in Fig. 2b ($t = 50$ ms; F -statistic, Comparisons among channel time series for asynchrony subsets, $p < 0.0001$; see “[Materials and methods](#)”). These marked differences vanished at $t = 200$ ms (Fig. 2b, second column). A second channels cluster showed significant differences across subsets between 306 and 330 ms (Fig. 2b, third column; F -statistic, Comparisons among channel time series for asynchrony subsets, $p < 0.05$ see “[Materials and methods](#)”), but only the comparison between $Q = 1$ and $Q = 4$ yielded a significant difference (t -statistic, Comparisons among

channel time series for asynchrony subsets, $p < 0.003$; see “[Materials and methods](#)”). Scalp activations still showed small differences at 400 ms, but they were not statistically significant (Fig. 2b, fourth column). At $t = 500$ ms the scalps from all asynchrony subsets were very similar (Fig. 2b, fifth column).

Much of the differences between subsets of asynchronies appear in the frontal region. Particularly, Fig. 2c, d, show the differential Fz dynamic for $Q = 1$ and $Q = 4$ for $T_n = 667$ ms and $T_n = 444$ ms, respectively. Around 100 ms after the stimulus occurrence, only negative asynchronies ($Q = 1$) displayed a positive activation. At 200 ms, both subsets of synchronization errors peaked. Probably, this “fixed” potential is related with an auditory component while the first peak ($t = 100$ ms) shifts with the motor response. Both periods display similar dynamics but the traces of the shorter period are not so well-defined.

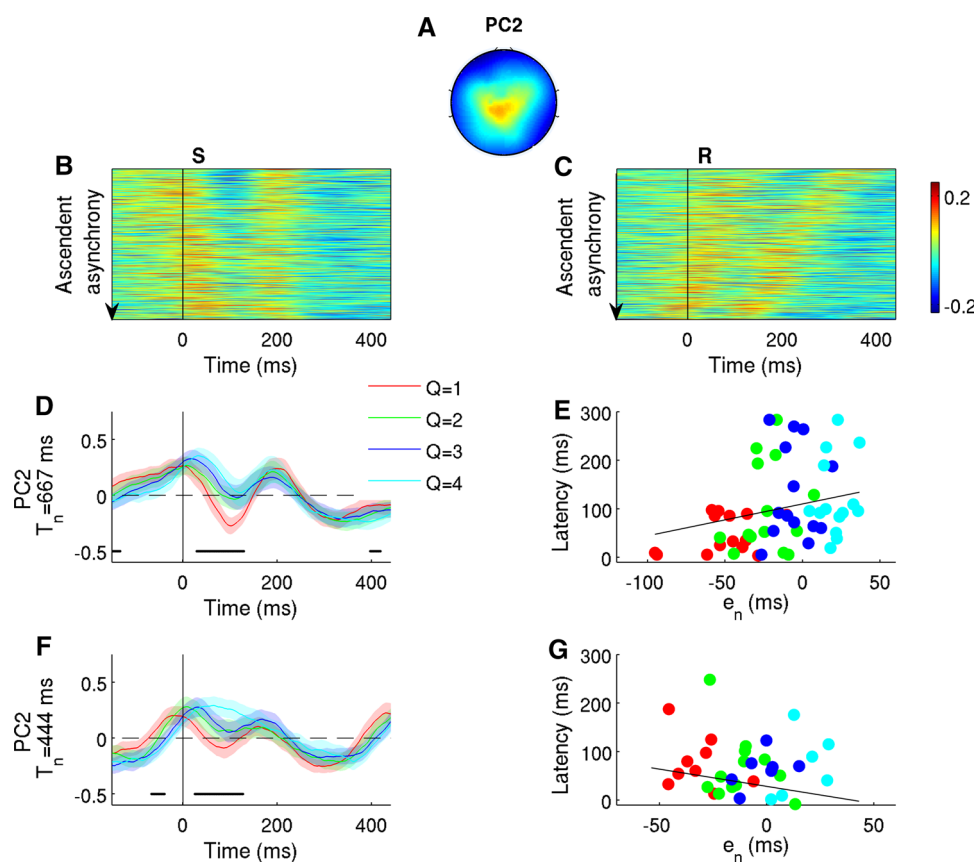


Fig. 4 First negative peak of the second Principal Component (PC2) identifies the asynchrony. **a** Scalp topography of PC2 for $T_n = 667$ ms (4 % of the variance). **b, c** PC2 activations from stimulus- and response-aligned data for $T_n = 667$ ms (projection of all epochs sorted by increasing asynchrony and averaged across subjects). **d, f** PC2 activations grouped by asynchrony subset for $T_n = 667$ ms and $T_n = 444$ ms, respectively (*thick line* mean; *shaded region* standard error). Stimulus-aligned data, projected onto PC2 and averaged within asynchrony subsets and across all subjects. The *solid black horizontal*

segments identify time windows where the difference between traces was significant (comparisons among PC projections, $p < 0.01$ during 19 ms, see “Materials and methods”). **e, g** Correlation between median of asynchrony subset and PC2 first peak latency for $T_n = 667$ ms and $T_n = 444$ ms, respectively. The correlation between latency and median of asynchronies was not significant for both periods ($T_n = 667$ ms: $R^2 = 0.2$, $p = 0.18$; $T_n = 444$ ms: $R^2 = -0.26$, $p = 0.08$)

PCA and dimensionality reduction

In order to explore in-depth the differences among asynchrony subsets and among timepoints found in Fig. 2, we performed a Principal Component (PC) Analysis (see “Materials and methods”). The first two principal components explained 91 and 4 % of the variance, respectively, for $T_n = 667$ ms (78 and 15 % of the variance for $T_n = 444$ ms); the third component explained less than 1 % of the variance for both periods and the amplitude of the projections were very small, so we decided to focus on the first two. Voltage scalp topographies of principal components 1 (PC1) and 2 (PC2) for the longer period are displayed in Figs. 3a, 4a, respectively. The correlation coefficient between PC1 for $T_n = 444$ ms and $T_n = 667$ ms was 0.9 with $p < 0.001$ (we obtained a similar result for PC2).

First principal component: combined stimulus-locked and response-locked potentials

PC1 had a fronto-central activation (Fig. 3a) whose topography resembled the evoked potential at $t = 50$ ms after the auditory stimulus in the $Q = 1$ subset (Fig. 2b, top row). Figure 3b, c display the stimulus- and response-aligned projection of all trials onto PC1 for $T_n = 667$ ms (ordered by asynchrony and averaged across subjects). A two-peak activation pattern appears, with the first peak approximately locked to response occurrence and the second peak locked to stimulus occurrence. In order to test this, we projected the four data subsets onto PC1 (Figs. 3d, f, for both periods); the traces displayed significant differences (black segments): between $t = -10$ ms and $t = 180$ ms (Comparisons among PC projections, $p < 0.01$ during 19 ms; see “Materials and methods”). Note that

Fig. 5 PC2 predicts the asynchrony value at the next step. All traces locked to the stimulus occurrence at step n ($t = 0$). **a, b** PC2 data for $T_n = 444$ ms and $T_n = 667$ ms, respectively, from asynchrony subset $Q(n) = 1$ grouped by the asynchrony subset at the next step $Q(n + 1)$: red indicates keeping the same subset $Q(n + 1) = 1$ (“no jump”); green means transition to either $Q(n + 1) = 3$ or 4 (“jump”). **c, d** PC2 data for $T_n = 444$ ms and $T_n = 667$ ms, respectively, from $Q(n) = 4$ grouped by asynchrony subset at the next step $Q(n + 1)$: red means keeping the same subset $Q(n + 1) = 4$ (“no jump”); green means transition to either $Q(n + 1) = 1$ or 2 (“jump”). Gray vertical bars identify the significant time window observed in Fig. 4. Solid gray horizontal segments identify time windows where significant differences between red and green traces occur ($p < 0.05$ during 17 ms, comparisons among PC projections)

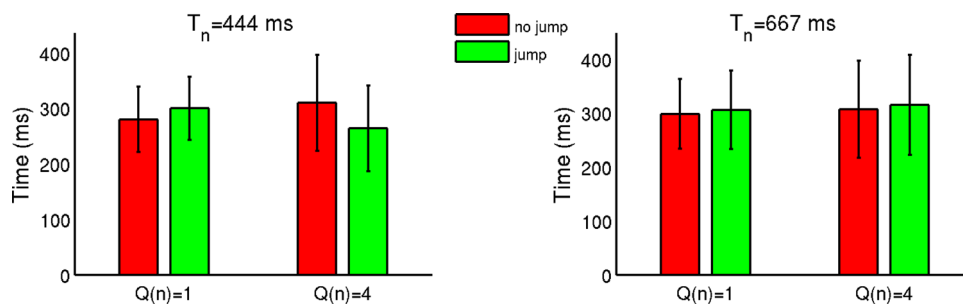
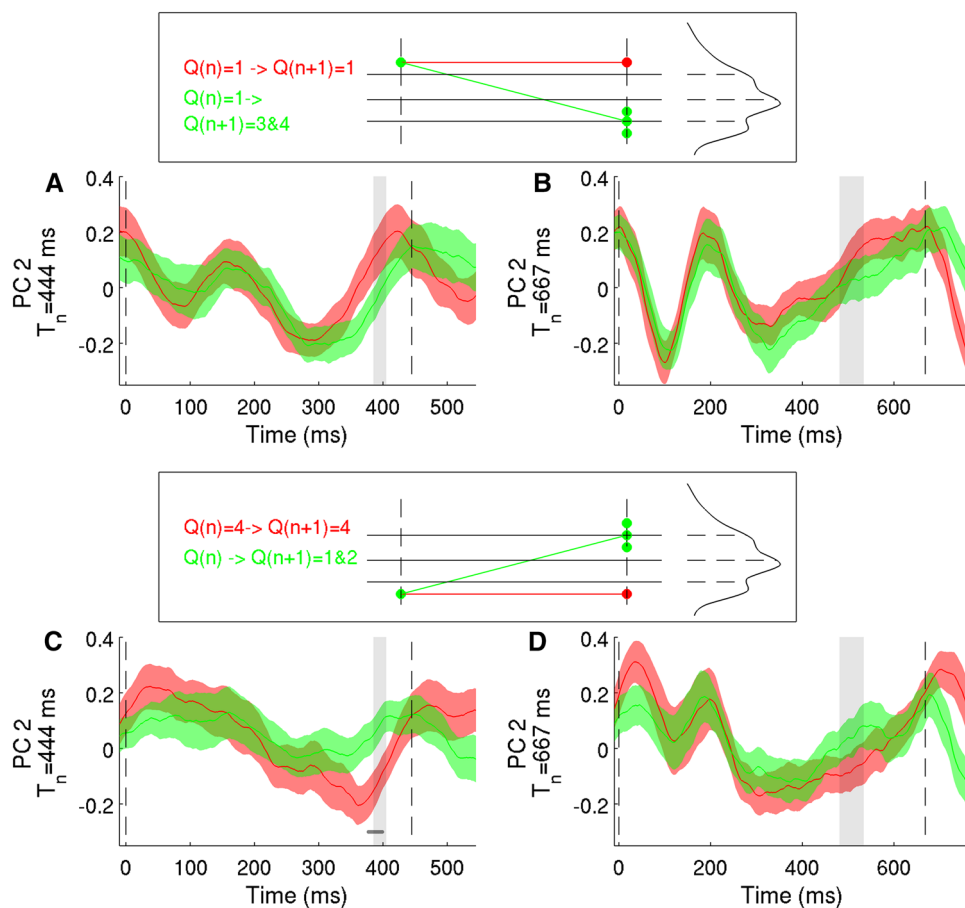


Fig. 6 A fixed marker for the evaluation of the asynchrony: PC2 ramp onset time for all experimental conditions. A three-way, $2 \times 2 \times 2$, repeated-measures ANOVA does not yield significant results (see “Materials and methods”, comparisons among ramp

onsets), meaning that the positive-going ramp starts always at the same time after the stimulus, independent of stimulus period and asynchrony subset at consecutive steps $Q(n)$ and $Q(n + 1)$. The mean ramp onset time is (298 ± 10) ms (mean \pm SEM)

these time windows include the timepoints where we found significant differences in the raw data in Fig. 2b, thus supporting our choice of PCA to investigate the origin of those differences.

Within these time windows, the time trace of $Q = 1$ (red curve) displayed two distinct peaks, roughly at $t = 66$ and 200 ms after stimulus onset, while the time trace of $Q = 4$ (cyan curve) displayed only one peak at around $t = 200$ ms. The time traces of $Q = 2, 3$ displayed a

smooth crossover between the other two, with the first peak decreasing in amplitude and increasing in latency and the second peak keeping amplitude and position. This suggests that PC1 represents overlapping processes time-locked to either the stimulus occurrence (the fixed peak at $t = 200$ ms) or the response occurrence (the shifting peak). This hypothesis was further supported by a significant correlation between latency (see “Materials and methods”, “Latency analysis”) and the median value of the

asynchrony subset for every subject (Fig. 3e; colors labeling subsets; every subject is represented by four points red–green–blue–cyan; $R^2 = 0.57$, $p < 0.001$).

As in the dynamic of Fz, the projections for the shorter period look very similar to the ones of the longer period (Fig. 3f) although the latency analysis was not significant. This negative result could be due to the greater overlapping of the peaks for the shorter period (lack of well-defined activations).

Asynchrony and the amplitude of the second principal component

As shown in the previous paragraph, correlations between stimulus or response occurrences and latencies of cortical activations were strong and showed up in the largest of principal components, PC1. On the other hand, projections onto PC2 appeared to vary in amplitude rather than in latency. Figure 4b, c show the stimulus- and response-aligned projection of all trials onto PC2 for $T_n = 667$ ms (ordered by asynchrony and averaged across subjects), with a negative peak appearing roughly around 100 ms after the stimulus; the projection of the four data subsets onto PC2 (Fig. 4d, f) showed significant differences occurring at the negative peak between 30 and 130 ms (Comparisons among PC projections, $p < 0.01$ during 19 ms; see “Materials and methods”). This negative peak was mostly aligned to the stimulus occurrence, as can be seen by comparing the traces in Fig. 4b, c, and as quantified by a non-significant correlation between latency and asynchrony for both periods (Fig. 4e, g).

We performed an ANOVA to compare the absolute amplitude of the peak ($p < 0.01$, Comparisons among single peaks; see “Materials and methods”), with the result that amplitude of $Q = 1$ is significantly different from those of the other subsets. Even though the shorter period data behaved similarly, the ANOVA was not significant. As we suggest above, the shorter period displays a greater overlapping of peaks giving no significant results. Figure 4 suggests that the amplitude of the negative peak of PC2, occurring at 100 ms after the current stimulus, encodes the asynchrony associated with that stimulus, particularly distinguishing subset $Q = 1$ from the others.

PC2 displays a second time window with a significant difference among asynchrony subsets. The difference is located before the stimulus occurrence ($T_n = 444$ ms: $(-60, -40)$ ms and $T_n = 667$ ms $(-187, -132)$ ms). For the longer period this time window is repeated after the stimulus occurrence. These significant timepoints could be a consequence of the next asynchrony or could be associated with the previous subsets of synchronization errors.

Second principal components: two consecutive stimuli analysis

To understand the source of the significant difference of PC2 before the stimulus occurrence we expanded our analysis to two consecutive stimuli. We grouped the data according to whether the recorded asynchrony stayed in the same subset Q at consecutive steps n and $n + 1$ or changed subset (“jump” or “no jump”, see schemes in Fig. 5; see “Materials and methods”). We compared between groups with the same $Q(n)$, and thus any difference would be associated with the asynchrony subset at the following step $Q(n + 1)$.

The overall shape of the time traces of PC2 displayed the negative peak near 100 ms for both periods with $Q(n) = 1$ (Fig. 5a, b) and a smaller peak for $Q(n) = 4$ (Fig. 5c, d) as expected (compare with Fig. 4d, f). Panel C showed significant differences between “jump” and “no jump” traces during the positive-going ramps in $Q(n) = 4$ (between $t = 377$ and $t = 394$ ms) for $T_n = 444$ ms (Comparisons among PC projections, see “Materials and methods”). This time window is similar to the one found in Fig. 4f (we explicitly pointed out these time windows with gray vertical bars). Both, for the shorter and longer period, as well as for the two subsets of $Q(n)$, the traces corresponding to the more negative asynchronies at step $n + 1$ are highest within these time points. Furthermore, negative asynchronies at step $n + 1$ display highest positive-going ramps. To contrast the amplitude across the ramps, we performed a global permutation test (see “Materials and methods”: comparisons for a single time-window) with statistically significant results for the shorter period ($p = 0.03$ for $Q(n) = 1$ and $p = 0.004$ for $Q(n) = 4$, Fig. 5a, c) and for the longer one ($p = 0.05$ for $Q(n) = 1$ and $p = 0.04$ for $Q(n) = 4$, Fig. 5b, d). Taking into account that $Q(n)$ is the same in every case, Fig. 5 suggests that positive-going ramp of PC2 gives information about the position of the next response.

Not surprisingly, the duration of the ramp was shorter in the data with $T_n = 444$ ms. Interestingly, the PC2 positive-going ramps appear to start always at the same time point after the previous stimulus, around 300 ms, not depending on the period of the sequence or the latency of the previous or next response. Figure 6 shows the onset of the PC2 ramp for every condition; a three-way, repeated measures ANOVA (Comparisons among ramp onsets, see “Materials and methods”) yielded non-significant results, meaning that for all conditions the PC2 positive-going ramp started always at around the same time, that is (298 ± 10) ms after the stimulus. The (mean \pm SEM) ramp onset time for the longer period was (306 ± 11) ms, and for the shorter period (290 ± 10) ms. Probably, a fixed time (independently of the

period length) is necessary to trigger the next response preparation.

Discussion

Even in the simplest paced finger-tapping task, which is tapping along an isochronous metronome, average synchronization has to be actively maintained by the nervous system by means of an error correction mechanism—otherwise, small differences between the interstimulus interval and the interresponse interval would accumulate and make the responses drift away from the stimuli. Indeed, when the subject is instructed to keep tapping at the same pace after the metronome has been muted (what is called a continuation paradigm), the “virtual asynchronies” computed between the continuing taps and the extrapolated silent beats usually get quite large within a few taps (Repp 2005), even for musically trained subjects. Thus, performance feedback—either in the form of timepoint differences, like the asynchrony, or time interval differences between metronome and taps—is crucial for the subject to maintain average synchrony.

The asynchrony and the difference between interstimulus and interresponse intervals are the two most prominent sources of performance feedback in finger tapping to a beat, according to behavioral observations and models (Michon & Van der Valk 1967; Wing & Kristofferson 1973a, b; Hary & Moore 1987; Mates 1994a, b; Pressing & Jolley-Rogers 1997; Large & Jones 1999; Vorberg & Schulze 2002; Praamstra et al. 2003; Schulze, Cordes, & Vorberg 2005). However, most of the EEG, MEG, fMRI, and TMS studies were designed either to find correlations between brain activity and acoustic properties or task parameters like baseline tempo (Dhamala et al. 2003; Lewis, Wing, Pope, Praamstra, & Miall 2004; Zanto, Snyder, & Large 2006), or to find brain regions involved in the behavior (Jancke, Loose, Lutz Specht & Shah 2000; Molinari et al. 2007; Pollok et al. 2008; Bijsterbosch et al. 2011). Instead, here we provide evidence to help achieve the ultimate goal of understanding how asynchronies, the most distinctive source of feedback to guide sensory-motor coordination in isochronous paced finger tapping, are used to dynamically sustain an accurate, non-drifting response sequence.

Neurophysiological signature of the asynchrony in the absence of perturbation

If the asynchrony is effectively one of the most important sources of temporal information about the performance, then soon after the asynchrony is defined—i.e. soon after

the last event, either tap or tone, occurs—a signature should appear in the neurophysiological markers either as a distinctive component latency or component amplitude which correlates with the size of the asynchrony (Müller et al. 2000).

A component whose latency shifts according to the size of the asynchrony, however, might be difficult to interpret as carrying information about the physiological representation of the asynchrony due to confounding. This is because one of the events that define the asynchrony will always shift in time too according to the size of the asynchrony, either with stimulus- or response-alignment of the data, thus making the correlation trivial (see Fig. 3d, f; see Müller et al. 2000, and the follow-ups (Pollok et al. 2003, Pollok, Müller, Aschersleben, Schnitzler, & Prinz 2004)).

We found that the amplitude of the negative peak of PC2 roughly at 100 ms after stimulus (Figs. 4d, f) carries information about the asynchrony in an isochronous setting. To our knowledge, this is the first report of a correlation between the observable asynchrony and a neurophysiological measure in isochronous finger tapping. Praamstra et al. (2003) recorded auditory-evoked EEG potentials (AEP) during synchronization to a sequence with phase-shift perturbations, and showed that the observed amplitude modulation of AEPs was correlated with the time course of the asynchrony but only for a few steps after the perturbation. Interestingly, there is a similarity between the voltage scalp distribution of the error-related negativity (ERN) shown in Praamstra et al. (2003) (Fig. 7b label 3 in that work) and our PC2 (Fig. 4a here, perhaps after adjusting the arbitrary sign that results from the computation of the principal components). Indeed, Praamstra and coworkers showed that an ERN only occurred after positive, large (+50 ms, supraliminal) perturbations. Notice that an unexpected, positive perturbation forces the subject to have a larger, negative asynchrony at the perturbation step (and at a few steps following it), which is consistent with our result that the amplitude of PC2 at $t = 100$ ms particularly distinguishes $Q = 1$ (i.e., the most negative asynchronies) from the other subsets. Our result, however, was obtained under isochronous conditions; thus, together with the result by Praamstra et al. (2003), it might confer a more general validity to the correlation between asynchrony and PC2 amplitude. This result supports the dynamical constraints we proposed in the building of the mathematical model for the error correction mechanism (Bavassi et al. 2013). In that work, we postulated that the recovery of asynchronies was commanded by a unique mechanism, independently from the source of the error. This model was successfully tested with different size and type of perturbations (step change, phase shift of event onset shift).

Asymmetry between positive and negative asynchronies

The prevailing view regarding the negative mean asynchrony (NMA) in the finger-tapping literature is that it reflects a point of subjective synchrony, which would only be established at the level of central representations after possible differences in peripheral and/or central processing times for the tap and the tone, explaining thus the well-established observation that taps precede the tones on average by about 20–80 ms (Aschersleben 2002). In absolute terms, however, the asynchronies corresponding to earlier and later taps are very different: because of the NMA, early taps yield normally large negative asynchronies, while the asynchronies for late taps can be close to zero. Similarly, negative perturbations of around the size of the NMA would make the asynchrony decrease in absolute terms, which would be in accordance with the finding by Praamstra et al. (2003) who demonstrated an ERN for large positive perturbations only. This normally asymmetric distribution of asynchronies produces a confound when considering any true asymmetry in the underlying mechanisms.

In our work, however, the NMA in 8 out of the 13 subjects was very close to zero (between -15 and 15 ms), and it was between -37 and 15 ms for all subjects, which led to individual asynchrony distributions mostly symmetric around the absolute zero for most of the subjects. In addition, all statistical tests in this work were performed according to a “within-subject” design; for instance, to test the statistical significance of the negative peak around 100 ms in PC2, the four subsets $Q = 1, 2, 3, 4$ were compared within each subject, thus eliminating the possibility of inadvertently counterbalancing among subjects with larger and smaller NMAs. These facts, together with our asymmetric result that PC2 amplitude around 100 ms distinguishes $Q = 1$ from the other asynchrony subsets, speaks against the argument that any asymmetry found in the neurophysiological traces is due to the distribution of asynchronies being normally shifted towards more negative values because of the NMA. We conclude, therefore, that our result in Figs. 4d and f reflects a true asymmetry around the median of the asynchrony distributions, i.e., around the so-called point of subjective synchrony.

There is an increasing amount of evidence of asymmetric behavior in paced finger-tapping tasks under perturbations. Repp (2002, 2011) showed that the amount of asynchrony correction at the first step after a phase-shift perturbation (called the Phase Correction Response, PCR) is smaller for negative than for positive perturbations, though only for perturbation magnitudes greater than 50 ms (10 % of the baseline period). Thaut et al. (1998) showed that the time series of the asynchrony in response

to a positive step-change perturbation of 10 % of the stimulus period exhibited considerable overshoot before approaching the new baseline, but not for negative perturbations where synchrony is recovered monotonically. This observation was made more systematic by Bavassi et al. (2013), where we performed small step-change perturbations (of up to 10 % of the baseline period) and showed that the amount of overshoot is zero for negative perturbations and it increases nonlinearly for positive perturbations. These reported asymmetric features of the behavior can be related to our finding that the amplitude of PC2 distinguishes the most negative asynchronies ($Q = 1$) from the other asynchrony subsets. In finger tapping to a beat, a corrective response does not involve activation or deactivation of a different effector, but rather a temporal adjustment in the activation of the same effector. It is possible that the computations needed to trigger a corrective tap earlier versus later are different, or at least that the same processes are shifted in time and thus overlap differently.

A fixed duration for the evaluation of the asynchrony

It is known that both the standard deviation and mean (in absolute value) of the asynchronies in an isochronous task increases linearly with the interstimulus interval (Repp 2003). This observation could lend support to the hypothesis that the error correction process works on a “relative” basis, adjusting its response and dynamics in proportion to the period of the sequence. We found a suggestive evidence of a predictor signal of the next response in the positive-going ramp, in Fig. 5. These ramps look to start always at a fixed point independently of the period or the asynchrony at $Q(n) = 1$, Fig. 6. These results suggest that the higher process of the asynchrony, and probably the error correction mechanism, finished at a fixed time after the tone: around 300 ms after the stimulus, i.e. the start time of the positive-going ramp in PC2.

In a very recent work, Hove, Balasubramaniam & Keller (2014) found that the Phase Correction Response (PCR) is an automatic adjustment that is constrained primarily by the time taken to integrate auditory and motor information, this process takes 250 ms. Besides, using single-neuron extracellular recordings in monkeys performing a related task, Merchant, Zarco, Pérez, Prado & Bartolo (2011) described five groups of neurons with a variety of activity profiles; some of them had features that did not depend on the stimulus period (e.g., ramping slope and ramp onset time in the “time-accumulator cells”). These findings together with our result support the alternative hypothesis that at least some of the neurophysiological processes underlying sensorimotor synchronization, likely overlapping in time, have

a fixed duration that does not depend on the size of the asynchrony or the interstimulus period.

It would be very interesting to find the relationship, if any, between the existence of fixed-duration processes and the known rate limits of sensorimotor synchronization (Repp 2005). Although tapping synchronization is possible with a metronome interval as short as 175 ms (Pressing & Jolley-Rogers 1997), previous works suggest that there is a change in the behavior for interval durations of less than 250–300 ms as evidenced by changes in the relationship between variability and metronome interval (Peters 1989; Repp 2005).

Predictability of the next asynchrony

Our results suggest that there might be differences in the processing of positive and negative asynchronies. Moreover, the PC2 projections for the analysis of the two consecutive stimuli show that the preceding positive-going ramp is a predictor of asynchronies at step $n + 1$ (Fig. 5). We found the traces that arrived to the negative errors in $Q(n + 1) = 1$ were higher than the others, independently of the period or the asynchrony at $Q(n)$. In other words, the height of the positive-going ramp correlates with the asynchrony on the subsequent step. Interestingly, the onset of this ramp is the same for the two periods and the two subsets $Q(n)$, (298 ± 10) ms. A possible explanation is that the predictor of next asynchrony reflects a motor preparation signal. Probably, this positive-going ramp is triggered after the processing of the previous asynchrony has finished. By the other hand, the height of the ramp could be a “footprint” of the error correction mechanism. More experiments are needed to distinguish between both explanations.

Overall, our study shows that the first two Principal Components give relevant information about the higher processing of the asynchrony in an isochronous finger-tapping task. This is a step forward towards the comprehension of the physiological processes in charge of sensorimotor synchronization, with the ultimate goal of unveiling the role of the sources of performance feedback like the asynchrony, its representation in the brain, and how the relevant neural computations in which it is involved are performed.

Acknowledgments We thank Manuel Eguía for technical support in the building of the Arduino shield, Laura Kaczer, Veronica Perez Schuster, Pablo Bartfeld and Martín Graziano for useful discussions. This work was funded by grant PICT 881/07 (Agencia Nacional de Promoción Científica y Tecnológica, Argentina), grant UNQ 53/3004 (Universidad Nacional de Quilmes, Argentina) and grant Milstein/Raíces (Ministerio de Ciencia y Tecnología, Argentina). M.S. is sponsored by CONICET and the James McDonnell Foundation 21st Century Science Initiative in Understanding Human Cognition—Scholar Award.

Compliance with ethical standards

Conflict of interest The authors declare that they have no conflict of interest.

Ethical approval All procedures performed in studies involving human participants were in accordance with the ethical standards of the institutional and/or national research committee and with the 1964 Helsinki declaration and its later amendments or comparable ethical standards.

Informed consent Informed consent was obtained from all individual participants included in the study.

References

- Aschersleben, G. (2002). Temporal control of movements in sensorimotor synchronization. *Brain and Cognition*, *48*(1), 66–79.
- Bavassi, L., Tagliazucchi, E., & Laje, R. (2013). Small perturbations in a finger-tapping task reveal inherent nonlinearities of the underlying error correction mechanism. *Human Movement Science*, *32*(1), 21–47.
- Bijsterbosch, J., Lee, K., Hunter, M., Tsoi, D., Lankappa, S., Wilkinson, I., ... Woodruff, P. (2011). The Role of the Cerebellum in Sub- and Supraliminal Error Correction during Sensorimotor Synchronization: Evidence from fMRI and TMS. *Journal of Cognitive Neuroscience*, *23*(5), 1100–1112.
- Brainard, D. (1997). The psychophysics toolbox. *Spatial Vision*, *10*(4), 433–436.
- Chen, Y., Ding, M., & Kelso, J. A. (2001). Origins of timing errors in human sensorimotor coordination. *Journal of Motor Behavior*, *33*(1), 3–8.
- Dehaene, S., Naccache, L., Cohen, L., Bihan, D. L., Mangin, J. F., Poline, J. B., & Riviere, D. (2001). Cerebral mechanisms of word masking and unconscious repetition priming. *Nature Neuroscience*, *4*(7), 752–758.
- Delorme, A., & Makeig, S. (2004). EEGLAB: An open source toolbox for analysis of single-trial EEG dynamics including independent component analysis. *Journal of Neuroscience Methods*, *134*, 9–21.
- Dhamala, M., Pagnoni, G., Wiesenfeld, K., Zink, C., Martin, M., & Berns, G. (2003). Neural correlates of the complexity of rhythmic finger tapping. *NeuroImage*, *20*, 918–926.
- Duda, R., Hart, P., & Stork, D. (2000). “Pattern Classification” (2nd ed.). New Jersey: Wiley.
- Hary, D., & Moore, G. (1987). Synchronizing human movement with an external clock source. *Biological Cybernetics*, *56*(5), 305–311.
- Hemmelmann, C., Horn, M., Reiterer, S., Schack, B., Süsse, T., & Weiss, S. (2004). Multivariate tests for the evaluation of high-dimensional EEG data. *Journal of Neuroscience Methods*, *139*(1), 111–120.
- Hove, M. J., Balasubramaniam, R., & Keller, P. E. (2014). The time course of phase correction: a kinematic investigation of motor adjustment to timing perturbations during sensorimotor synchronization. *Journal of Experimental Psychology: Human Perception and Performance*, *40*(6), 2243.
- Jancke, L., Loose, R., Lutz, K., Specht, K., & Shah, N. (2000). Cortical activations during paced finger-tapping applying visual and auditory pacing stimuli. *Cognitive Brain Research*, *10*, 51–66.
- Kamienkowski, J. E., Ison, M. J., Quiroga, R. Q., & Sigman, M. (2012). “Fixation-related potentials in visual search: a combined EEG and eye tracking study”. *Journal of Vision* *12*(7), 4.

- Large, E., & Jones, M. (1999). The dynamics of attending: How people track time-varying events. *Psychological Review*, *106*(1), 119.
- Lewis, P., Wing, A., Pope, P., Praamstra, P., & Miall, R. (2004). Brain activity correlates differentially with increasing temporal complexity of rhythms during initialisation, synchronisation, and continuation phases of paced finger tapping. *Neuropsychologia*, *42*, 1301–1312.
- Makeig, S., Bell, A. J., Jung, T. P., & Sejnowski, T. J. (1996). "Independent component analysis of electroencephalographic data." *Advances in neural information processing systems*, 145–151.
- Maris, E., & Oostenveld, R. (2007). Nonparametric statistical testing of EEG- and MEG-data. *Journal of Neuroscience Methods*, *167*, 177–190.
- Mates, J. (1994a). A model of synchronization of motor acts to a stimulus sequence. *Biological Cybernetics*, *70*(5), 463–473.
- Mates, J. (1994b). A model of synchronization of motor acts to a stimulus sequence. *Biological Cybernetics*, *70*(5), 475–484.
- Merchant, H., Zarco, W., Pérez, O., Prado, L., & Bartolo, R. (2011). Measuring time with different neural chronometers during a synchronization-continuation task. *Proceedings of the National Academy of Sciences*, *108*(49), 19784–19789.
- Michon, J. A., & Van der Valk, N. J. L. (1967). A dynamic model of timing behavior. *Acta Psychologica*, *27*, 204–212.
- Mognon, A., Jovicich, J., Bruzzone, L., & Buiatti, M. (2011). ADJUST: an automatic EEG artifact detector based on the joint use of spatial and temporal features. *Psychophysiology*, *48*(2), 229–240.
- Molinari, M., Leggio, M., & Thaut, M. (2007). The cerebellum and neural networks for rhythmic sensorimotor synchronization in the human brain. *The Cerebellum*, *6*(1), 18–23.
- Müller, K., Schmitz, F., Schnitzler, A., Freund, H., Aschersleben, G., & Prinz, W. (2000). Neuromagnetic correlates of sensorimotor synchronization. *Journal of Cognitive Neuroscience*, *12*(4), 546–555.
- Peters, M. (1989). The relationship between variability of intertap intervals and interval duration. *Psychological Research*, *51*(1), 38–42.
- Pollok, B., Gross, J., Kamp, D., & Schnitzler, A. (2008). Evidence for anticipatory motor control within a Cerebello-Diencephalic-Parietal Network. *Journal of Cognitive Neuroscience*, *20*(5), 828–840.
- Pollok, B., Müller, K., Aschersleben, G., Schmitz, F., Schnitzler, A., & Prinz, W. (2003). Cortical activations associated with auditorily paced finger tapping. *NeuroReport*, *14*(2), 247–250.
- Pollok, B., Müller, K., Aschersleben, G., Schnitzler, A., & Prinz, W. (2004). "The role of the primary somatosensory cortex in an auditorily paced finger tapping task." *Experimental Brain Research* *156*(1):111–117.
- Praamstra, P., Turgeon, M., Hesse, C., Wing, A., & Perryer, L. (2003). Neurophysiological correlates of error correction in sensorimotor-synchronization. *NeuroImage*, *20*(2), 1283–1297.
- Pressing, J., & Jolley-Rogers, G. (1997). Spectral properties of human cognition and skill. *Biological Cybernetics*, *76*(5), 339–347.
- Repp, B. (2002). Phase correction in sensorimotor synchronization: nonlinearities in voluntary and involuntary responses to perturbations. *Human Movement Science*, *21*(1), 1–37.
- Repp, B. (2003). Rate limits in sensorimotor synchronization with auditory and visual sequences: the synchronization threshold and the benefits and costs of interval subdivision. *Journal of Motor Behavior*, *35*(4), 355–370.
- Repp, B. (2005). Sensorimotor synchronization: a review of the tapping literature. *Psychonomic Bulletin & Review*, *12*(6), 969–992.
- Repp, B. (2011). Tapping in synchrony with a perturbed metronome: the phase correction response to small and large phase shifts as a function of tempo. *Journal of Motor Behavior*, *43*(3), 213–227.
- Repp, B. H., & Penel, A. (2002). Auditory dominance in temporal processing: new evidence from synchronization with simultaneous visual and auditory sequences. *Journal of Experimental Psychology: Human Perception and Performance*, *28*(5), 1085.
- Repp, B. H., & Su, Y. H. (2013). Sensorimotor synchronization: a review of recent research (2006–2012). *Psychonomic Bulletin & Review*, *20*(3), 403–452.
- Rodríguez-Fornells, A., Kurzbuch, A. R., & Münte, T. F. (2002). Time course of error detection and correction in humans: neurophysiological evidence. *The Journal of Neuroscience* *22*(22), 9990–9996.
- Schulze, H., Cordes, A., & Vorberg, D. (2005). Keeping synchrony while tempo changes: accelerando and ritardando. *Music Perception*, *22*(3), 461–477.
- Sigman, M., & Dehaene, S. (2008). Brain mechanisms of serial and parallel processing during dual-task performance. *The Journal of Neuroscience*, *28*(30), 7585–7598.
- Thaut, M., Tian, B., & Azimi-Sadjadi, M. R. (1998). Rhythmic finger tapping to cosine-wave modulated metronome sequences: evidence of subliminal entrainment. *Human Movement Science*, *17*(6), 839–863.
- Vorberg, D., & Schulze, H. (2002). Linear phase-correction in synchronization: predictions, parameter estimation, and simulations. *Journal of Mathematical Psychology*, *46*(1), 56–87.
- Wing, A., & Kristofferson, A. (1973a). Response delays and the timing of discrete motor responses. *Attention, Perception, & Psychophysics*, *14*(1), 5–12.
- Wing, A., & Kristofferson, A. (1973b). The timing of interresponse intervals. *Attention, Perception, & Psychophysics*, *13*(3), 5–12.
- Zanto, T., Snyder, J., & Large, E. (2006). Neural correlates of rhythmic expectancy. *Advances in cognitive psychology*, *2*(2–3), 221–231.